

Physicochemical Properties of Silibinin-Phosphatidylcholine Complex and its Implications for Drug Formulations

REENU PUNIA¹, C. SINGH^{1,3}, R. P. SINGH³, M. SINGH⁴ AND R. P. SINGH^{1,2*}

Cancer Biology Laboratory, School of Life Sciences, Jawaharlal Nehru University, New Delhi 110067, ¹School of Life Sciences, Central University of Gujarat, Gandhinagar, Gujarat 382030, ²Special Centre for Systems Medicine, Jawaharlal Nehru University, New Delhi 110067, ³Division of Food and Nutritional Biotechnology, National Agri-Food Biotechnology Institute (NABI), Sahibzada Ajit Singh (SAS) Nagar, Punjab 140306, ⁴School of Chemical Sciences, Central University of Gujarat, Gandhinagar, Gujarat 382030, India

Punia *et al.*: Physicochemical Properties of Silibinin-Phosphatidylcholine Complex

Silibinin, an active constituent of silymarin possesses several medicinal properties. Although, the poor water solubility and less bioavailability restrict the clinical utility of silibinin, the complex of silibinin and phosphatidylcholine manifested outstanding biological activities *in vivo*. Thereby, the complex of silibinin was prepared with phosphatidylcholine (1:2, w/w) for better solubility and therapeutic efficacy and their physicochemical properties were analyzed. Thermal analysis, nuclear magnetic resonance and Fourier transform infrared spectroscopy data revealed that complex of silibinin with phosphatidylcholine improved binding efficiency of silibinin with non-covalent interactions. Kinetics of *in vitro* drug release with high performance liquid chromatography analysis showed that complex of silibinin-phosphatidylcholine released maximum 30 %-32 % silibinin into phosphate-buffered saline between 3 h to 6 h at pH 3 and 7 at 37°. Release profile of silibinin from silibinin-phosphatidylcholine complex in Swiss albino mice suggested that the complex increased silibinin concentration three times more in plasma samples of mice than individual silibinin treatment after 10 d. Furthermore, no significant changes were observed in body weight and diet consumption of mice throughout the study. Therefore, the study suggested that complex of silibinin-phosphatidylcholine improves the solubility and bioavailability of silibinin, which explains better efficacy and clinical potential of silibinin in its complex form against various disorders including cancer.

Key words: Silibinin, phosphatidylcholine, physicochemical, activation energy, bioavailability

Silymarin, isolated from *Silybum marianum* has been used to treat various diseases for hundreds of years^[1]. Silibinin, a most active constituent of silymarin, is known for its hepatoprotective^[2], antioxidative^[1], antidiabetic^[3], hypocholesterolemic, cardioprotective^[4,5], chemopreventive, neuroprotective and anticancer activities^[6]. Despite of having a good therapeutic profile, an inefficient intestinal absorption due to poor solubility of silibinin restricts its uses into the biological system^[7]. For example, after oral administration of 120 mg/kg of silibinin in healthy volunteers at T_{max} 1 h-2 h, C_{max} in plasma was only 1.1-1.3 $\mu\text{g/ml}$ ^[8]. In rats, silibinin has only 0.95 % absolute oral bioavailability^[9]. This condition warranted the further investigation for improving the bioavailability of silibinin.

There are several ways to improve the bioavailability of drugs. In recent past, nanoencapsulation and self-emulsifying drug delivery systems have attracted the pharmaceutical companies for efficient absorption of

many therapeutics drugs. Other solutions to increase the absorption of silymarin include modification of drug with salts, esters and complexation with cyclodextrins or phospholipids, nanoemulsions, biodegradable polymeric nanoparticles biocompatible polymers^[7]. To improve the clinical uses of silibinin by counteracting its less bioavailability, low solubility and absorption, various formulations have been prepared. These synthesized derivatives include silybin-N-methyl-glucamine, silybin bis-hemisuccinate, silybin-11-O-phosphate, β -cyclodextrin complex and silybin-phosphatidylcholine^[10].

This is an open access article distributed under the terms of the Creative Commons Attribution-NonCommercial-ShareAlike 3.0 License, which allows others to remix, tweak, and build upon the work non-commercially, as long as the author is credited and the new creations are licensed under the identical terms

*Address for correspondence

E-mail: rana_singh@mail.jnu.ac.in

Accepted 04 August 2022

Revised 27 September 2021

Received 09 June 2021

Indian J Pharm Sci 2022;84(4):979-987

Silybin-Phospholipid Complex (SB-PC) complex was previously made and its biological activities were tested^[11]. In a recent study, it is observed that the complex improves the bioavailability of silibinin in healthy and volunteers with chronic liver disease. In animal model, SB-PC is also known to reduce lipid peroxidation, collagen accumulation, oxidative stress and liver damage^[10]. Nevertheless, analyzing the physicochemical property of SB-PC complex is yet to be determined.

In the present study, the physicochemical properties of SB-PC complex are determined and subsequently release profile of SB from the complex was analyzed *in vitro* and *in vivo* system to evaluate the causes of improved bioavailability and efficacy of SB in its complex form.

MATERIALS AND METHODS

Silibinin (98 % purity), acetone, Dimethyl Sulfoxide (DMSO), acetic acid and Potassium bromide (KBr) were purchased from Sigma-Aldrich, United States of America (USA). Phospholipon 90 G containing 94 %-102 % phosphatidylcholine (purified from soybean lecithin) was provided by Lipoid, Switzerland. The other chemical reagents were of analytical grade.

Measurement of surface tension and viscosity:

Five different concentrations of silibinin including 0.0, 3.3, 10, 33.33, 100 and 300 μM were prepared with DMSO (0.1 %) and PC (1:2, w/w) by using water as solvent. Surface tension and viscosity of all the formulations of SB were measured at 37° by using Borosil Mansingh Survisimeter, which was calibrated by calibration constant. For surface tension (γ), pendent drop was counted and surface tension was calculated by the equation 1:

$$\gamma = (n^0/n) (\rho/\rho^0) \gamma \dots\dots\dots(1)$$

Where γ^0 is surface tension of reference (water) at 37°, n^0 and n are pendent drop numbers of reference and sample, ρ and ρ^0 are density of sample and reference, respectively^[12].

Viscosity (η) was measured by putting the value of measured flow time of sample in the following equation

$$\eta = \eta^0 (t/t^0) (\rho/\rho^0) \dots\dots\dots(2)$$

Where η^0 is viscosity of reference at 37°, t and t^0 are flow time of sample and reference, respectively^[12].

Measurement of density, sound velocity and activation energy:

Density and sound velocity of all given formulations

of SB was measured by advance density and sound velocity meter (DSA 5000 M, Anton Paar). Instrument was adjusted with Milli-Q water at 37° prior to analyzing samples. Activation energy was calculated as the method described by Singh *et al.*, 2010^[12].

Preparation of SB-PC complex:

After the initial screening, the complex of SB-PC was prepared as per the method described by Duan *et al.*^[13]. In brief, SB and PC in 1:2 ratios were mixed in round bottom flask, which was dissolved into acetone until the solution become transparent. Then, the complex was refluxed at 50° for 2 h and acetone was evaporated under vacuum at 50°. Dried residues of the complex were collected and placed into vials in desiccator at room temperature.

Construction of standard calibration curve of silibinin and determination of the content of silibinin in SB-PC complex:

Different concentrations of silibinin were dissolved into 40 % methanol and run through High Performance Liquid Chromatography (HPLC). The HPLC system was consisted of Flexar Ultraviolet (UV)/Visible (Vis) LC detector, Flexar binary LC pump, PerkinElmer Shelton, USA. Chromatographic separation was attained with Supelco, Ascentis C₁₈ (150 mm×4.6 mm, 5 μm) column. The method for HPLC analysis was adopted from Singh *et al.*, 2002^[14]. The retention time of SB was observed 23.5±0.4 min.

Content of SB in SB-PC complex was determined by preparing 100 μM solution of complex in 40 % methanol. After complete dissolution of sample, 20 μl of sample was injected into HPLC and SB contents in the complex was calculated by the equation 3;

$$\text{Content (\%)} = (\text{SB content in PC}) / (\text{Used amount of SB}) \times 100 \dots\dots\dots(3)$$

Differential Scanning Calorimetry (DSC):

Physical properties of SB, PC and SB-PC were evaluated with DSC. The sealed samples in aluminum crimp cell were heated at the rate of 5°/min by using DSC 6000 PerkinElmer. Continuous flow of nitrogen was maintaining the steady state. The heat flow was 30°-250° for SB, 30°-300° for PC and SB-PC complex.

Fourier Transform Infrared Spectroscopy (FTIR):

Attenuated Total Reflectance (ATR)-FTIR spectra of SB, PC and SB-PC complex was analyzed by using a PerkinElmer (Spectrum 100) FTIR spectrometer. Prior to

data acquisition, the optical bench was purged with dry nitrogen to minimize external interference and total of 60 scans were collected for each run at a resolution of 4 cm^{-1} . All samples used for FTIR analysis were lyophilized and well mixed with KBr and all spectra were recorded at 25° .

Nuclear Magnetic Resonance (NMR) analysis:

^1H and ^{13}C -NMR spectra of SB, PC and SB-PC complex were recorded on Bruker Avance III 500 MHz spectrometer equipped with a broadband Broad Band Fluorine Observation (BBFO) probe. Chemical shifts Delta (δ) are mentioned in parts per million (ppm) using residual solvent signal (DMSO-d6) as a reference.

In vitro drug release:

The *in vitro* release pattern of the SB from SB-PC complex was performed according to method described by Mohammadi *et al.*, with some modifications^[15]. In brief, 10 mg of complex (containing $30\ \mu\text{M}$ of SB in SB-PC) was placed into the vessels with 250 ml of Phosphate Buffer Saline (PBS) of pH 3.0 (mimicking stomach pH) and pH 7.0 (intestinal pH) at 37° . To enhance the solubility of SB, 0.3 % Sodium Dodecyl Sulphate (SDS, w/v) was added into the PBS and placed the vessels into shaking water bath at 120 rpm at 37° . After the specific time interval, 1.5 ml of supernatant was removed by using $0.20\ \mu\text{m}$ syringe filter and injected into C_{18} column by using same method as described earlier. After each sampling, equal volume of the fresh PBS was passed through the same filtration. The concentration of the released SB was analyzed by comparing the area of the peak of released drug with standard SB curve.

In vivo drug release study:

To further evaluate the release of SB from PC complex, male Swiss albino mice (~ 10 w old) were housed in the Central Laboratory Animal Resources (CLAR), which was approved by Institutional Animal Ethics Committee, Jawaharlal Nehru University, New Delhi, India. The mice were provided with standard food pellets and drinking *ad libitum* water and kept at 12 h light/12 h dark cycle at controlled temperature ($25^\circ \pm 1^\circ$) with 60 %-70 % humidity. The mice were divided randomly into six groups and treated daily with respective doses of drug complex prepared in base solution (0.9 % Sodium chloride (NaCl), 1 % Tween 20, 3 % ethanol, 6.6 mM Sodium hydroxide (NaOH)) by oral administration. From the day of treatment, mice were monitored daily for their body weight, food and water consumption for any sign of toxicity. On 10th d, after ~ 3 h of respective treatments, blood sample was collected from tail vein

and centrifuged immediately at 3000 rpm for 10 min to get the plasma. All the plasma samples were stored at -20° for further analysis.

Silibinin concentration in mice plasma were detected by using HPLC. The small amount of plasma sample was vortex-mixed with chilled acetonitrile (1:2 volume ratio) followed by centrifugation at 12 000 g for 10 min. An aliquot of supernatant ($20\ \mu\text{l}$) was injected directly into HPLC column and analyzed with the method mentioned above.

Statistical analysis:

Statistical significance of the data was performed using SigmaPlot 8.0 software. The statistical significance of difference between control group and treated groups was determined with Student's t-test. $p < 0.05$ was considered as statistically significant.

RESULTS AND DISCUSSION

We have screened different concentrations of SB (3.3-300 μM) with 0.1 % DMSO and PC (1:2 w/w) using water as a solvent and measured their surface tension, viscosity, density and sound velocity. Water molecules bind to each other through cohesive forces. SB did not cause any significant change in surface tension, viscosity, density and sound velocity of water due to its poor solubility. Similarly addition of 0.1 % DMSO and PC (1:2, w/w) in water system also had not caused any significant changes in these parameters.

The interaction between two molecules affects the activation energy of the sample. Bonding of DMSO molecules with water utilized more energy of the solution as compared to PC and decreased the value of activation energy, however, different concentration of SB did not cause any change in activation energy of solution.

Additionally, PC is known to improve the bioavailability of SB and thus to understand the cause of this effect, complex of SB with PC was prepared with 1:2, w/w ratio on the basis of reported studies by Singh *et al.*^[16]. The HPLC analysis confirmed the content of SB in SB-PC complex, which was 68.1 %.

DSC curve analysis of SB, PC and SB-PC explained the formation of the complex as compared to their parent components (fig. 1). Multi-ring structure of SB degraded at 171.03° with a broad endothermic peak. While PC showed a prominent melting peak at 255.90° with a transition onset at 237.89° , a known melting peaks of nonpolar alkyl chain and polar head of PC. Multiple endothermic scratches in the PC explained about certain compounds like nonpolar lipids or water that could be

present in form of impurities. Interestingly, melting temperature of SB-PC complex was drastically shifted than their pure forms as shown in fig. 1a-fig. 1c, giving an impression that SB-PC complex was successfully formed.

FTIR spectra of SB, PC and SB-PC complex were analyzed by using KBr disk method (fig. 2). FTIR spectra of SB revealed the presence of Hydroxyl (-OH) group at 3449 cm^{-1} with -CH aromatic stretch at 2947 cm^{-1} . We also observed C=C stretching in SB at 1369 cm^{-1} ^[17,18] and presence of C=O group at 1647 cm^{-1} ^[19,20]. PC contained some moisture, which gave a broad -OH band at the starting of Infrared Spectroscopy (IR) spectrum as reported previously^[21]. Absorption bands at wave number of 2923 cm^{-1} (H-O-H), 2854 cm^{-1} (>CH-) and 1736 cm^{-1} (CH₃-C=O) were present in PC^[22]. Alkyl groups were observed in between 1500 to 600 cm^{-1} in the IR spectrum. While, in the SB-PC complex, -OH and CH₃-C=O group of SB were disappeared, which inferred the possibility of hydrogen bonding between SB and PC. Additionally, the shifting of the absorption frequency in lower region of FTIR suggested about hydrophobic interaction of aromatic rings of SB to PC in the complex.

¹H and ¹³C-NMR allowed characterizing SB, PC and SB-PC complex. Chemical shift observed in ¹H and ¹³C-NMR of PC suggested the use of the structure of PC having unsaturated aryl chain (fatty acid) (fig. 3a- fig. 3c and fig. 4a- fig. 4c). These chemical shifts of PC observed were corresponding to previous reports^[23-25]. Likewise, ¹H NMR of SB matched with a report published by Fazio *et al.*^[26]. Chemical shift observed in ¹³C-NMR of SB were assigned accordingly to Kellici *et al.*^[27]. Whilst in case of ¹H-NMR of SB, proton associated with benzene and heterocyclic rings was observed in between δ 6.8 to 7.2 and 4.9 to 5.9 ppm, respectively. Peak of 1,4 dioxane was observed at around δ 3.75 ppm.

Chemical shifts present in SB-PC complex were nearly identical to those of its constituents. Nevertheless, chemical shifting in ¹H-NMR of some peaks of SB was observed, especially those which were nearer with -OH, -O- and =O groups. These changes clearly indicate that these groups are involved in the complexation with PC (fig. 3). An eminent characteristic of complex is that peaks of aromatic and heterocyclic regions were broader from their own peaks as compared to the complex, which may be interpreted for the reduction of resonance behavior in mixture.

In vitro analysis revealed that complex of SB with PC released maximum drug between 3 h to 6 h, whereas

pure SB did not dissolve completely even after 48 h (fig. 5a). Low solubility of pure SB in phosphate buffer solution was supported by the study done by Sahibzada *et al.*^[28]. PC released 31.39 % SB at pH 3.0 and 32.14 % at pH 7.0. When compared to pH 7.0, pH 3 facilitated earlier release of SB from the complex, which could be evident from earlier 0.02 h (fig. 5b). This may be due to destabilizing hydrogen and van der waals interaction. These observations suggested that PC have capacity to enhance the bioavailability SB at lower pH that mimics the stomal condition.

Low bioavailability of SB has been a major concern by various research group, which make them to prepare different formulations of SB^[9,29]. Since SB-PC complex released maximum drug in desirable time and pH *in vitro*, we also examined for *in vivo* release profile of SB in Swiss albino mice. Briefly, mice were fed daily with SB alone and its complex with PC. After 10 d of treatment, mice blood was collected and analyzed for the level of free SB. After ~3 h of oral administration, SB-PC complex released three times more SB compared to SB alone (100 μM) (fig. 6a). We also compared release profile of SB-PC complex even at less concentrations such as 33.3 and 66.7 μM and observed 0.5 and 2 fold increase in release of free SB, respectively, as compared to 100 μM SB. There was no considerable change in body weight and diet consumption among the groups during the experiments (fig. 6b and fig. 6c). This study suggested that the better release of SB can be achieved through the administration of SB-PC complex form, which could lead to its better absorption in intestine and bioavailability of drug in mice plasma or blood circulation as compared to its alone treatment.

In the present study, physicochemical properties of SB-PC complex were measured. DSC and FTIR studies conformed the proper binding of SB to PC and suggested for non-covalent interactions such as hydrogen bonding or van der waals forces between them. Furthermore, chemical shift observed in SB-PC complex when compared with either SB or PC alone supported the formation of complex as observed with FTIR. PC facilitated better release and higher dissolution of SB as compared to pure SB. *In vivo* release of SB in its complex with PC further increased the bioavailability of free SB in mice plasma as compared to SB individual treatment. Thus SB-PC improves therapeutic profile of SB and may help to explain and support the higher efficacy of the complex against many diseases and its clinical utilization.

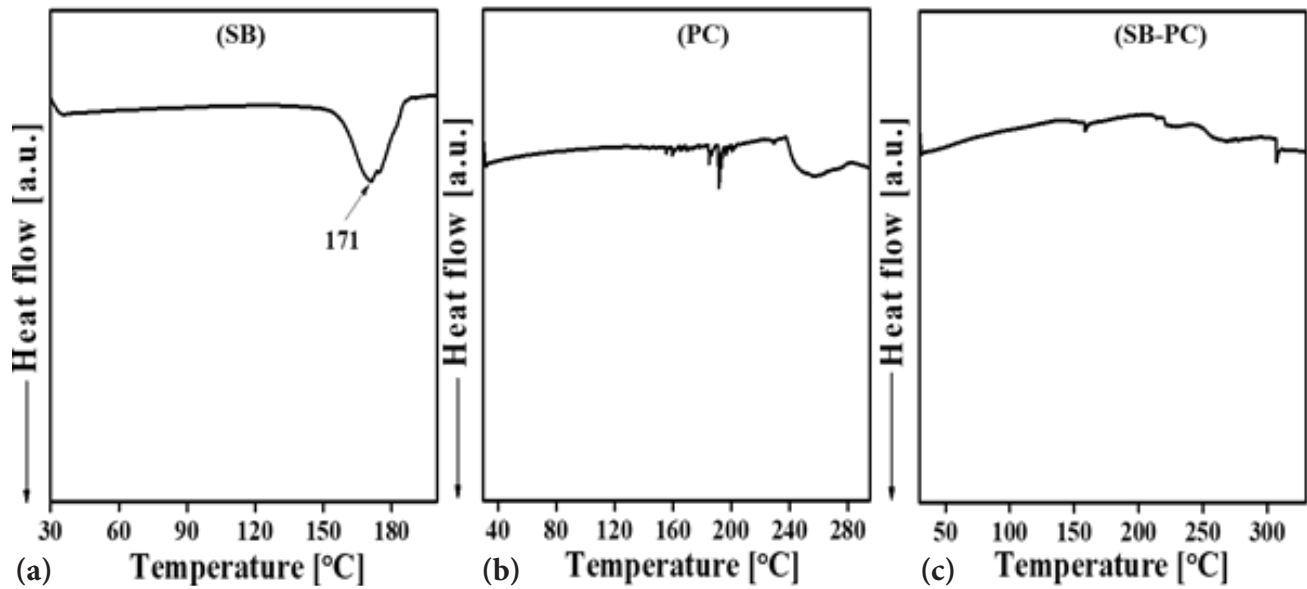


Fig. 1: DSC thermogram of SB, PC and SB-PC complex

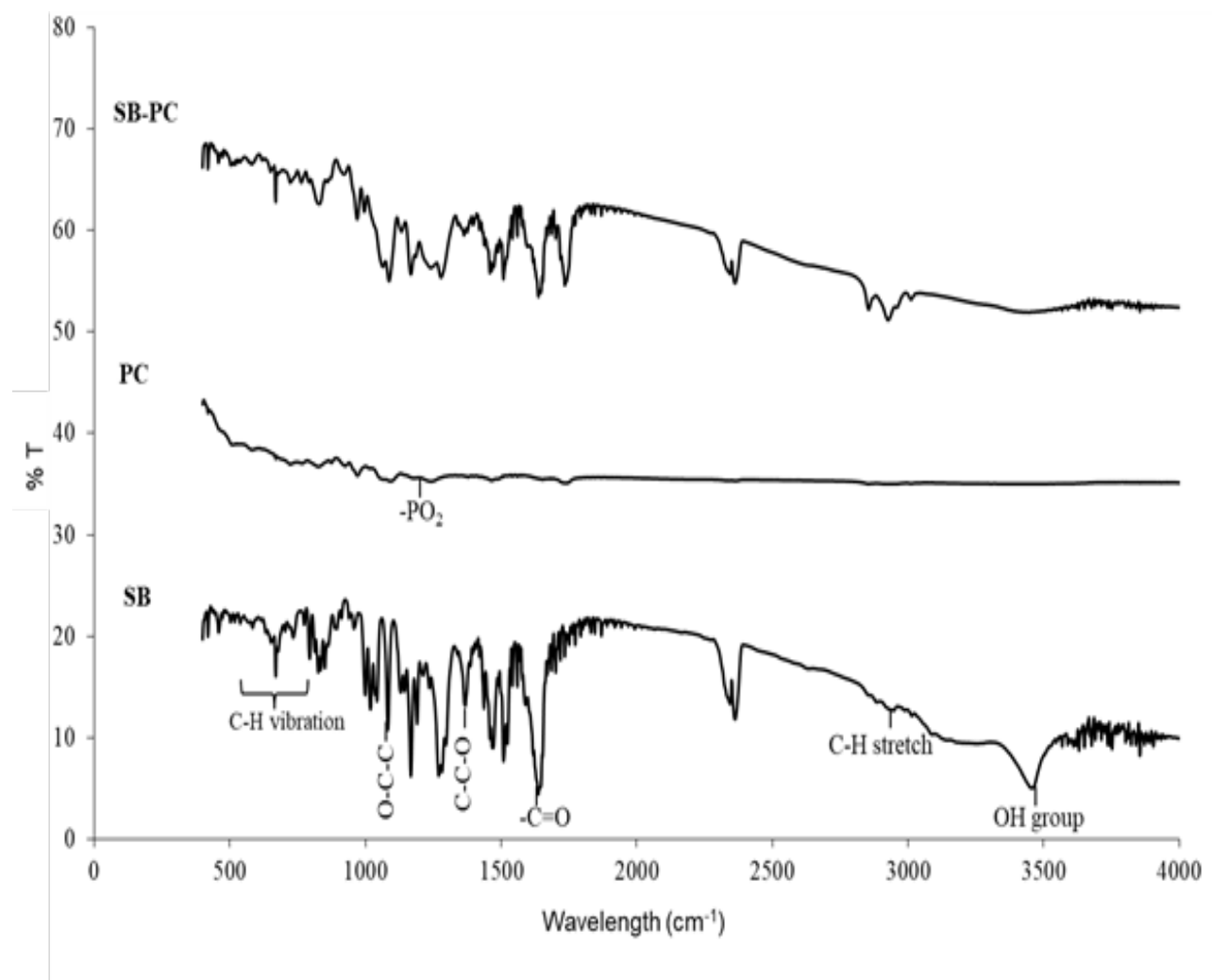


Fig. 2: FTIR spectra of SB, PC and SB-PC complex

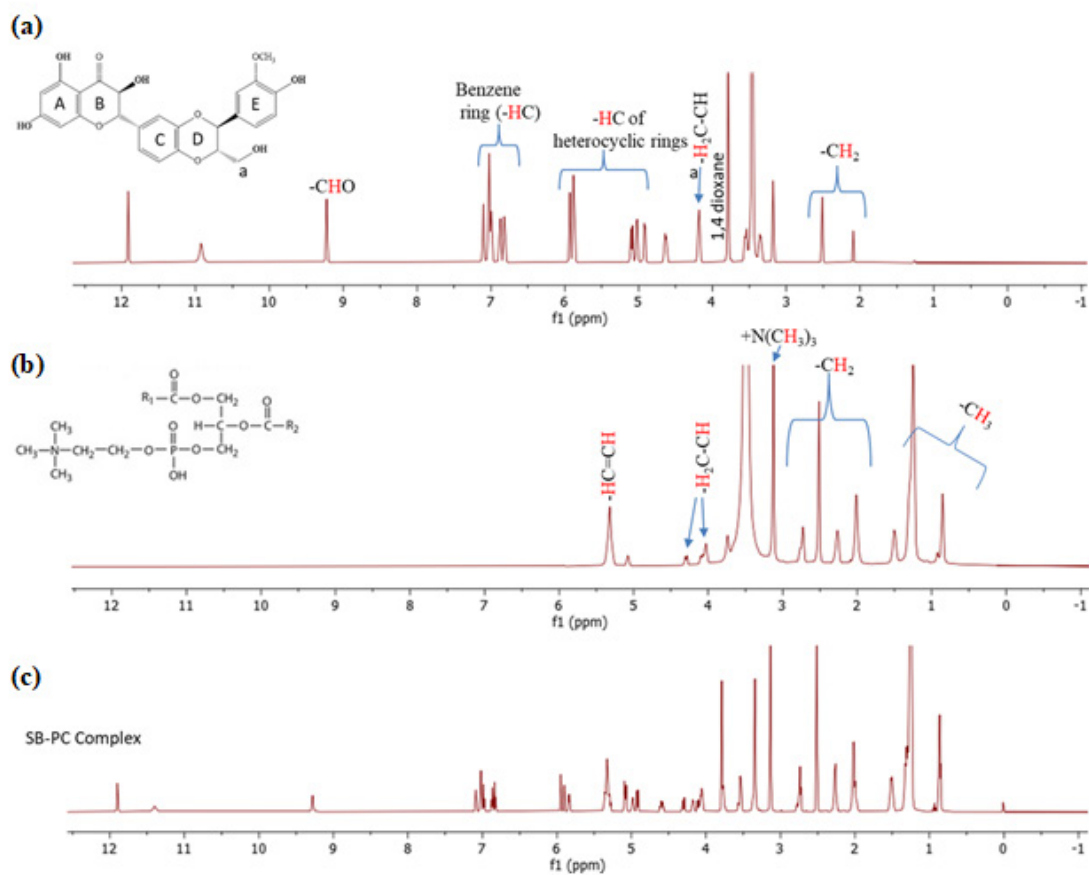


Fig. 3: ^1H , spectra of SB (a): PC; (b): SB-PC complex and (c): All spectra were recorded with DMSO-d_6

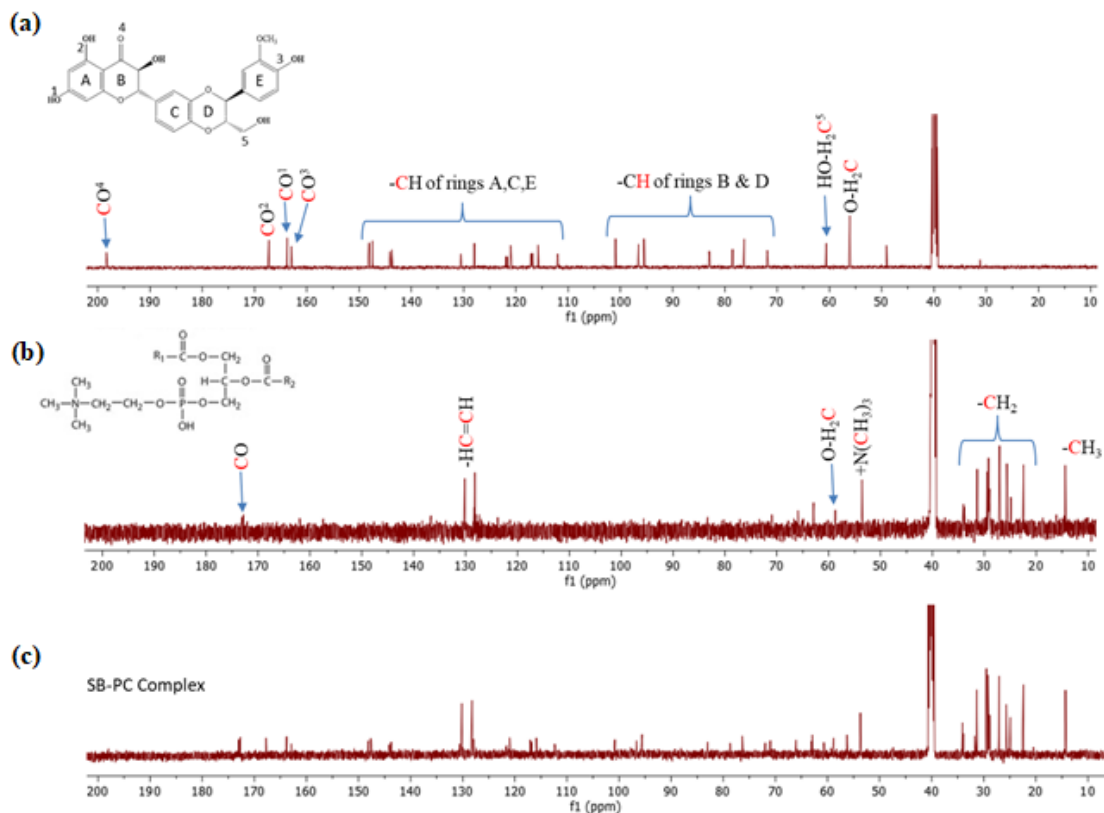


Fig. 4: ^{13}C , spectra of SB (a): PC; (b): SB-PC complex and (c): All spectra were recorded with DMSO-d_6

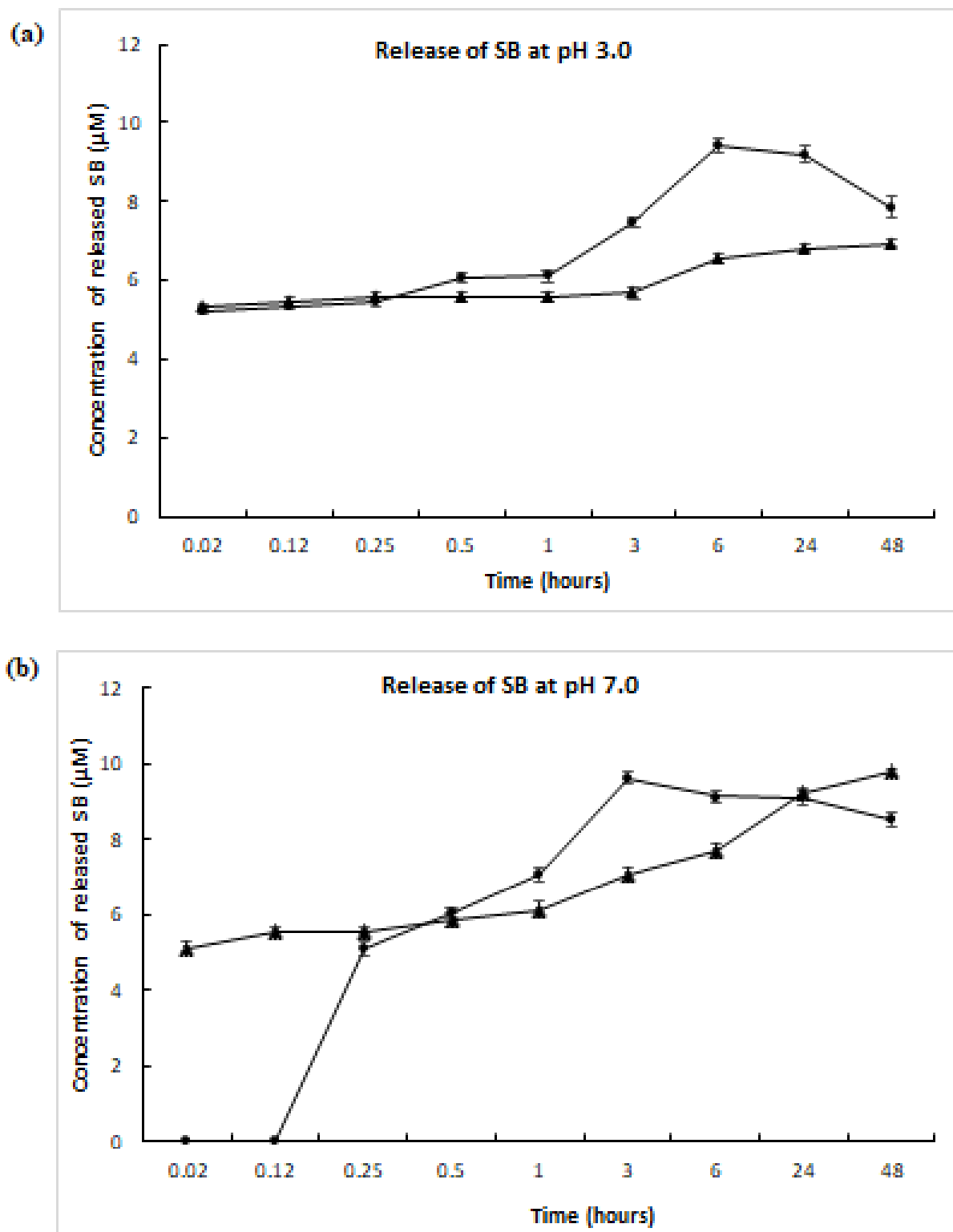


Fig. 5: *In vitro* release profile of SB in complex with PC at (a): pH 3.0 and (b): pH 7.0 were calculated and plotted against time
 Note: The data are presented as mean±Standard Error of the Mean (SEM) of triplicate samples for each group, (▲): SB only and (●): SB-PC

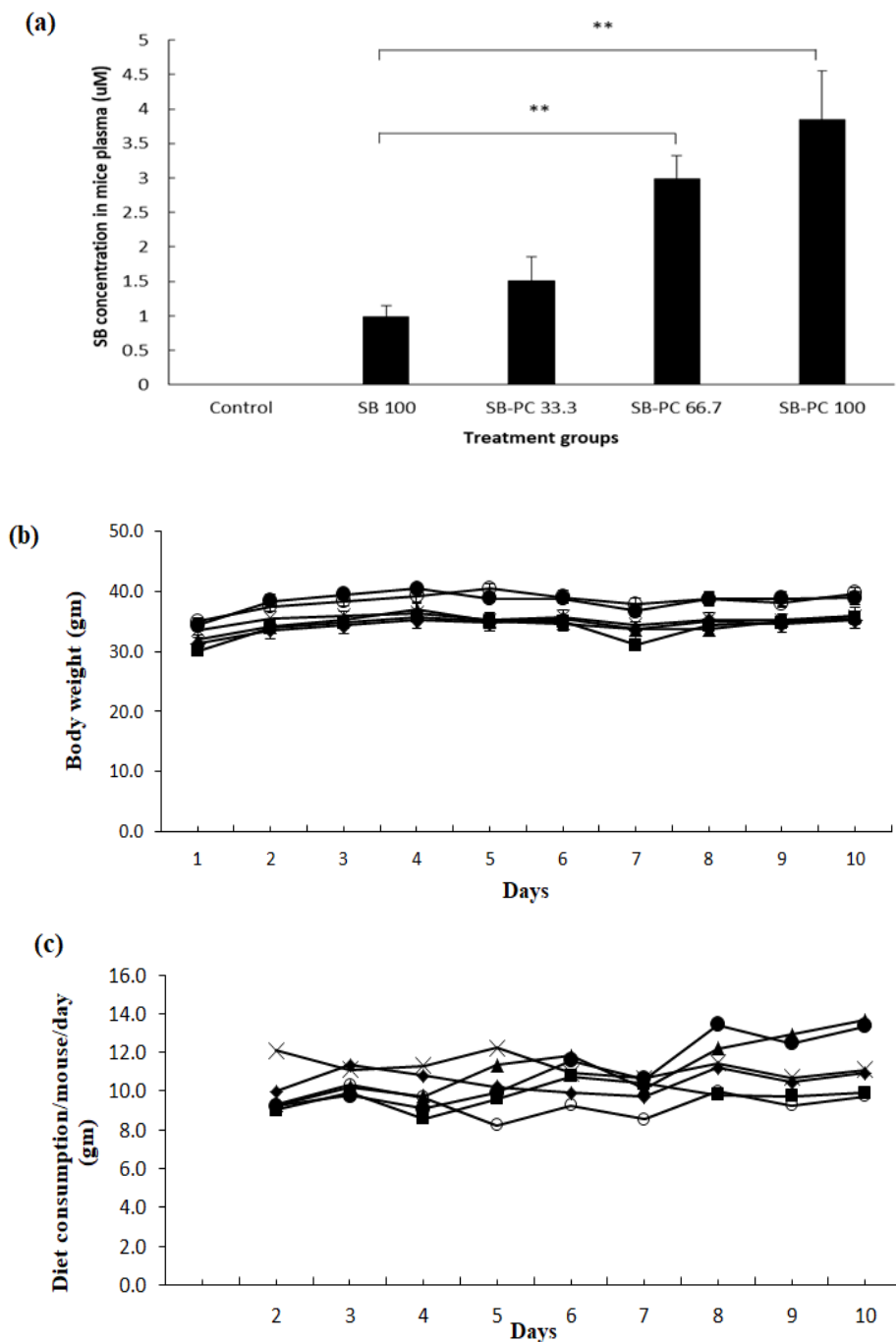


Fig. 6: Distribution of free SB in mice plasma. Total amount of free SB in mice plasma (a): Body weight per mouse and (b and c): Average diet consumption per mouse/day

Note: (a): Each data point represents mean of 3-6 replicate measurements with 20 µl sample; (b and c): Data are shown in means±SEM from 6 mice in each group. All the doses are in µM. Bars, SE; p<0.05, (—●—): Control; (—◆—): SB 50; (—▲—): SB 100; (—○—): SB-PC 33.33; (—×—): SB-PC 66.66 and (—■—): SB-PC 100

Acknowledgements:

We are thankful to Lipoid, Switzerland for providing us a gift sample of Phospholipon 90 G containing 94 %-102 % phosphatidylcholine. We acknowledge the UGC for providing fellowship supported to Reenu Punia and Chandrajeet Singh. We are grateful to the services of AIRF, JNU and financial support from DST-PURSE, UGC-RN, UPE-2, CUG and JNU.

Conflict of interests:

The authors declare that they have no conflicts of interests.

REFERENCES

- Gillessen A, Schmidt HH. Silymarin as supportive treatment in liver diseases: A narrative review. *Adv Ther* 2020;37(4):1279-301.

2. Delmas D, Xiao J, Vejux A, Aires V. Silymarin and cancer: A dual strategy in both in chemoprevention and chemosensitivity. *Molecules* 2020;25(9):2009.
3. Liu K, Zhou S, Liu J, Wang Y, Zhu F, Liu M. Silibinin attenuates high-fat diet-induced renal fibrosis of diabetic nephropathy. *Drug Des Devel Ther* 2019;13:3117-26.
4. Ramasamy K, Agarwal R. Multitargeted therapy of cancer by silymarin. *Cancer Lett* 2008;269(2):352-62.
5. Zhang T, Kawaguchi N, Yoshihara K, Hayama E, Furutani Y, Kawaguchi K, *et al.* Silibinin efficacy in a rat model of pulmonary arterial hypertension using monocrotaline and chronic hypoxia. *Respir Res* 2019;20(1):79.
6. You Y, Chen L, Wu Y, Wang M, Lu H, Zhou X, *et al.* Silibinin promotes cell proliferation through facilitating G1/S transitions by activating drp1-mediated mitochondrial fission in cells. *Cell Transplant* 2020;29:0963689720950213.
7. di Costanzo A, Angelico R. Formulation strategies for enhancing the bioavailability of silymarin: The state of the art. *Molecules* 2019;24(11):2155.
8. Kim YC, Kim EJ, Lee ED, Kim JH, Jang SW, Kim YG, *et al.* Comparative bioavailability of silibinin in healthy male volunteers. *Int J Clin Pharmacol Ther* 2003;41(12):593-6.
9. Wu W, Zu Y, Wang L, Wang L, Li Y, Liu Y, *et al.* Preparation, characterization and antitumor activity evaluation of silibinin nanoparticles for oral delivery through liquid antisolvent precipitation. *RSC Adv* 2017;7(86):54379-90.
10. Méndez-Sánchez N, Dibildox-Martinez M, Sosa-Noguera J, Sánchez-Medal R, Flores-Murrieta FJ. Superior silybin bioavailability of silybin-phosphatidylcholine complex in oily-medium soft-gel capsules vs. conventional silymarin tablets in healthy volunteers. *BMC Pharmacol Toxicol* 2019;20(1):1-6.
11. Barzaghi N, Crema F, Gatti G, Pifferi G, Perucca E. Pharmacokinetic studies on IdB 1016, a silybin-phosphatidylcholine complex, in healthy human subjects. *Eur J Drug Metab Pharmacokinet* 1990;15(4):333-8.
12. Singh M, Kumar V, Kale RK, Jain CL. Molecular activation energies ($\Delta\mu^*$) of L-lysine, L-tyrosine, L-proline, dl-alanine, glycerol, orcinol, iodine, DTAB and TMSOI for blending with melamine-formaldehyde-polyvinylpyrrolidone polymer resin illustrated with SEM. *J Appl Polym Sci* 2010;118(2):960-8.
13. Duan RL, Sun X, Liu J, Gong T, Zhang ZR. Mixed micelles loaded with silybin-polyene phosphatidylcholine complex improve drug solubility. *Acta Pharmacol Sin* 2011;32(1):108-15.
14. Singh RP, Dhanalakshmi S, Tyagi AK, Chan DC, Agarwal C, Agarwal R. Dietary feeding of silibinin inhibits advance human prostate carcinoma growth in athymic nude mice and increases plasma insulin-like growth factor-binding protein-3 levels. *Cancer Res* 2002;62(11):3063-9.
15. Mohammadi G, Nokhodchi A, Barzegar-Jalali M, Lotfipour F, Adibkia K, Ehyaei N, *et al.* Physicochemical and anti-bacterial performance characterization of clarithromycin nanoparticles as colloidal drug delivery system. *Colloids Surf B Biointerfaces* 2011;88(1):39-44.
16. Singh RP, Raina K, Sharma G, Agarwal R. Silibinin inhibits established prostate tumor growth, progression, invasion and metastasis and suppresses tumor angiogenesis and epithelial-mesenchymal transition in transgenic adenocarcinoma of the mouse prostate model mice. *Clin Cancer Res* 2008;14(23):7773-80.
17. Patel P, Raval M, Sheth N. Silibinin loaded solid lipid nanoparticles: Effect of different lipids and surfactants on physicochemical properties of nanoparticle. *Int J Pharm Investig* 2020;10(3):332-8.
18. Tan JM, Karthivashan G, Arulselvan P, Fakurazi S, Hussein MZ. Characterization and *in vitro* sustained release of silibinin from pH responsive carbon nanotube-based drug delivery system. *J Nanomater* 2014;2014:1-10.
19. Munajad A, Subroto C. Fourier transform infrared (FTIR) spectroscopy analysis of transformer paper in mineral oil-paper composite insulation under accelerated thermal aging. *Energies* 2018;11(2):364.
20. Omer AM, Ziora ZM, Tamer TM, Khalifa RE, Hassan MA, Mohy-Eldin MS, *et al.* Formulation of quaternized aminated chitosan nanoparticles for efficient encapsulation and slow release of curcumin. *Molecules* 2021;26(2):449.
21. Singh RP, Shukla MK, Mishra A, Kumari P, Reddy CR, Jha B. Isolation and characterization of exopolysaccharides from seaweed associated bacteria *Bacillus licheniformis*. *Carbohydr Polym* 2011;84(3):1019-26.
22. Singthong J, Cui SW, Ningsanon S, Goff HD. Structural characterization, degree of esterification and some gelling properties of Krueo Ma Noy (*Cissampelos pareira*) pectin. *Carbohydr Polym* 2004;58(4):391-400.
23. Alexandri E, Ahmed R, Siddiqui H, Choudhary MI, Tsiafoulis CG, Gerathanassis IP. High resolution NMR spectroscopy as a structural and analytical tool for unsaturated lipids in solution. *Molecules* 2017;22(10):1663.
24. Monakhova YB, Betzgen M, Diehl BW. ¹H NMR as a release methodology for the analysis of phospholipids and other constituents in infant nutrition. *Anal Methods* 2016;8(41):7493-9.
25. Niezgoda N, Gliszczynska A, Gładkowski W, Kempńska K, Wietrzyk J, Wawrzeńczyk C. Phosphatidylcholine with cis-9, trans-11 and trans-10, cis-12 conjugated linoleic acid isomers: Synthesis and cytotoxic studies. *Aust J Chem* 2015;68(7):1065-75.
26. Fazio E, Scala A, Grinato S, Ridolfo A, Grassi G, Neri F. Laser light triggered smart release of silibinin from a PEGylated-PLGA gold nanocomposite. *J Mater Chem B* 2015;3(46):9023-32.
27. Kellici TF, Ntountaniotis D, Leonis G, Chatziathanasiadou M, Chatzikonstantinou AV, Becker-Baldus J, *et al.* Investigation of the interactions of silibinin with 2-hydroxypropyl- β -cyclodextrin through biophysical techniques and computational methods. *Mol Pharm* 2015;12(3):954-65.
28. Sahibzada MU, Sadiq A, Khan S, Faidah HS, Khurram M, Amin MU, *et al.* Fabrication, characterization and *in vitro* evaluation of silibinin nanoparticles: An attempt to enhance its oral bioavailability. *Drug Des Devel Ther* 2017;11:1453-64.
29. Rad AH, Asiaee F, Jafari S, Shayanfar A, Lavasanifar A, Molavi O. Poly (ethylene glycol)-poly (ϵ -caprolactone)-based micelles for solubilization and tumor-targeted delivery of silibinin. *Bioimpacts* 2020;10(2):87-95